Comparative Analysis of Extended Kalman Filter and Unscented Kalman Filter for Simplified Vehicle Localization System

HARI PRASANTH S.M.
hpsvm@kth.se

January 15, 2024

Abstract

In the rapidly evolving domain of autonomous vehicles, achieving precise localization within their environment remains a pivotal challenge. Utilizing sensors such as GPS and IMU facilitates this localization, but direct reliance on raw sensor values may lack accuracy due to various influencing factors. To overcome this limitation, estimation methods, notably the Extended Kalman Filter (EKF) and Unscented Kalman Filter (UKF), have garnered attention. This research conducts a comparative analysis of the EKF and UKF algorithms in a simplified vehicle localization system, focusing on their performance in the presence of unmeasured state variables—a critical consideration for real-world applications. Using the KITTI dataset, the study illuminates the strengths and weaknesses of EKF and UKF in the chosen simplified system. In contrast to prevailing literature, the research findings consistently demonstrate the superiority of the EKF over the UKF across diverse datasets and noise levels. This disparity is attributed to the system's reduced complexity, where the EKF's precise approximation of non-linearity surpasses the UKF's reliance on sigma points, introducing inaccuracies in specific scenarios. In conclusion, this study emphasizes the efficacy of the Extended Kalman Filter over the Unscented Kalman Filter in simplified non-linear systems, offering valuable insights for the selection of estimation algorithms in similar applications.

1 Introduction

In the expanding realm of autonomous vehicles, a pivotal challenge is accurately localizing the vehicle within its environment. While global positioning systems (GPS) facilitate global localization, sensors such as inertial measurement units (IMU) and LiDAR play a crucial role in locally localizing the vehicle. In applications with lower computational demands, like navigation guidance similar to Google Maps, reliance on GPS and IMU sensors alone is common. However, the integration of GPS and IMU data becomes imperative to mitigate the inherent noise in these sensors and enhance localization precision [1].

The integration of GPS and IMU data alone, though, falls short of achieving highly precise positioning. To address this limitation, estimation methods come into play, utilizing sensor data and incorporating control inputs such as vehicle acceleration and steering. Real-world systems, being inherently non-linear, pose a everlasting challenge for estimation methods. The research in this domain has yielded various approaches, with Extended Kalman Filter (EKF) and Unscented Kalman Filter (UKF) emerging as two prominent methods. Notably, these methods, though both applicable to non-linear systems, adopt contrasting methodologies.

EKF, aims to linearize non-linear systems around their mean [2], while UKF, utilizes sigma points to capture the Gaussian spread of non-linear systems [3], yielding more robust estimation results. In this study, we opt for a simplified and approximated system, relative to the intricacies of real-world applications, to compare and evaluate the performance of EKF and UKF. A noteworthy aspect under scrutiny is the behavior of these estimation methods when one of the state variables is entirely unmeasured.

1.1 Contribution

Through the outcomes of this research, we aim to draw insightful comparisons between EKF and UKF using the Kitti dataset [4], shedding light on their respective strengths and weaknesses in the context of the selected simplified system. This exploration holds significance in enhancing our understanding of these estimation methods and their applicability, especially in scenarios where certain state variables remain unobserved.

1.2 Outline

After introducing the problem of autonomous vehicle localization, the report proceeds with a thorough examination of the related study area, offering insights into prior research. Subsequently, the methodology section unfolds, starting with an explanation of motion and measurement models and progressing to the implementation of Extended Kalman Filter (EKF) and Unscented Kalman Filter (UKF) for the chosen system. This systematic presentation sets the stage for the results and analysis section, where a critical evaluation of EKF and UKF performance under specified conditions is conducted.

The highlight of the report lies in the results and analysis, providing a comprehensive examination of the research findings. The conclusion section follows, summarizing key takeaways and emphasizing the broader significance of the research within the field of autonomous vehicle localization.

2 Related Work

In the domain of localization, extensive research has delved into comparing various estimation methods and enhancing filters for specific applications. Notably, relevant studies provide insights into the performance of filters under diverse scenarios.

A study by Konatowski et al. [5] titled ”Comparison of Estimation Accuracy of EKF, UKF, and PF Filters” investigates the accuracy of Extended Kalman Filter (EKF), Unscented Kalman Filter (UKF), and Particle Filter (PF) in maneuvering object location estimation. By employing simulations, the research concludes that UKF exhibits superior accuracy over EKF, particularly in handling second-order moments, while emphasizing PF’s significance for non-Gaussian distributions.

Giannitrapani et al.'s research [6] titled "Comparison of EKF and UKF for Spacecraft Localization via Angle Measurements" focuses on comparing EKF and UKF for spacecraft localization without range measurements, relying solely on angles-only measurements of celestial bodies. This study addresses the challenge of precise spacecraft self-localization in GPS-denied scenarios. While similar to our research, it differs by employing a dynamic spacecraft model considering gravitational effects and errors, using onboard sensors for elevation and azimuth measurements, and evaluating estimation methods based on the variance of the estimates.

In a study by Allotta et al. [7], titled "A Comparison between EKF-based and UKF-based Navigation Algorithms for AUVs Localization," the performance of EKF and UKF in localizing Autonomous Underwater Vehicles (AUVs) is explored. The research, conducted with Typhoon-class AUVs during sea missions, demonstrates the superiority of UKF over EKF in terms of localization accuracy. Despite similarities to our work in evaluating EKF and UKF, the study focuses on underwater scenarios with specific sensor setups.

Unlike the aforementioned studies, our research uniquely concentrates on a simplified autonomous vehicle motion model. Utilizing real-world ground truth data with added noise, the performance of EKF and UKF is assessed under conditions where one state variable is entirely unobserved. This distinctive aspect adds a novel perspective to filter evaluation, offering insights into their performance in scenarios with incomplete state observations.

3 Method(s)

This study leverages the KITTI dataset, a renowned benchmark in computer vision and autonomous driving research [4]. This dataset offers a rich and demanding array of real-world data, encompassing high-resolution images, lidar scans, and meticulously annotated ground truth, thus serving as a valuable resource for the evaluation and enhancement of localization and perception algorithms in autonomous systems. Specifically, our research focuses on the utilization of GPS and IMU data, in conjunction with the corresponding ground truth values. For further details on the dataset's structure, please refer to the documentation [8].

3.1 Motion model formulation

In order to streamline data processing and emphasize the implementation of the filtering technique, several assumptions have been introduced. One key simplification involves treating the z-axis position (altitude) as constant throughout the dataset, effectively reducing the system to a two-dimensional plane. The state variables governing the system are denoted as $[x, y, \theta]$, where x and y represent the vehicle's position, and θ signifies the vehicle's orientation or heading. The control inputs injected into the system consist of linear velocity, denoted as v, and angular velocity, denoted as ω.

The formulation of the system's motion model is guided by equation 5.9 from "Probabilistic Robotics" by Thrun [9]. This model, characterized as a velocity motion model, encapsulates the dynamic behavior of the vehicle. The model can be expressed through the following equations:

$$\begin{bmatrix} x_t \\ y_t \\ \theta_t \end{bmatrix} = \begin{bmatrix} x_{t-1} - \frac{v_t}{\omega_t}\sin\theta_{t-1} + \frac{v_t}{\omega_t}\sin(\theta_{t-1} + \omega_t \Delta t) \\ y_{t-1} + \frac{v_t}{\omega_t}\cos\theta_{t-1} - \frac{v_t}{\omega_t}\cos(\theta_{t-1} + \omega_t \Delta t) \\ \theta_{t-1} + \omega_t \Delta t \end{bmatrix} + \varepsilon_t \tag{1}$$

These equations intricately define the relationship between the state variables [x, y, θ] and the control inputs v and ω. Here, Δt is the time difference between $(t-1, t]$ and ε_t represents the process noise. The Gaussian noise term ε follows a distribution $\varepsilon \sim \mathcal{N}(0, R)$, where R denotes the process noise covariance matrix.

3.2 Experimental setup

The ground-truth GPS data, represented by longitude, latitude, and altitude, extracted from the dataset undergo a transformation into Earth-Centered-Earth-Fixed (ECEF) coordinates denoted as x, y, and z. This conversion is facilitated by the equations presented in Hofmann-Wellenhof et al. [10]:

$$\begin{bmatrix} x \\ y \\ z \end{bmatrix} = \begin{bmatrix} (N+h)\cos\phi\cos\lambda \\ (N+h)\cos\phi\sin\lambda \\ \left(\frac{b^2}{a^2}N+h\right)\sin\phi \end{bmatrix} \tag{2}$$

In the context of these equations, the variables are defined as follows: a represents the semi-major axis of the ellipsoid, b represents the semi-minor axis, ϕ represents latitude, λ represents longitude, and h represents altitude. The variable N assumes the role of the radius of curvature in the prime vertical, computed as $\frac{a}{\sqrt{1-e^2\sin^2\phi}}$, where e represents the eccentricity of the ellipsoid. Subsequently, the x, y, and z coordinates are transformed into the East-North-Up coordinate system, with the initial values serving as the reference point.

3.3 Measurement model formulation

For the measurement model, direct utilization of the GPS values proved challenging due to complications arising from the conversion between World Geodetic System (WSG) and XYZ coordinates, including the associated Jacobian. Given the time constraints, the approach shifted to using the directly converted XYZ values for the measurement model. Consequently, the measurement model adopts a linear and simplified form:

$$z_t = \begin{bmatrix} x_t \\ y_t \end{bmatrix} + \delta_t \tag{3}$$

Here, δ_t represents the measurement noise, adhering to a distribution $\delta \sim \mathcal{N}(0, Q)$, with Q denoting the measurement noise covariance matrix.

3.4 Extended Kalman Filter Implementation

This section explains the implementation of the Extended Kalman Filter (EKF) for estimating the system's state, encompassing the vehicle's position (x, y) and orientation (θ). The EKF algorithm, as outlined by Ribeiro et al. [2], unfolds through two main stages: the prediction step and the update step.

In the prediction step, the system state is forecasted using the motion model, and the corresponding covariance matrix is updated. The predicted state $\hat{\mathbf{x}}_t^-$ is computed using the motion model function $g(\hat{\mathbf{x}}_{t-1}, \mathbf{u}_t, \Delta t)$. The covariance matrix $\mathbf{P}_t^-$ is updated utilizing the first-order Jacobian of the motion model function ($\mathbf{G}_t$):

$$\hat{\mathbf{x}}_t^- = g(\hat{\mathbf{x}}_{t-1}, \mathbf{u}_t, \Delta t) \tag{4}$$

$$\mathbf{P}_t^- = \mathbf{G}_t \mathbf{P}_{t-1} \mathbf{G}_t^T + \mathbf{R}_t \tag{5}$$

The Jacobian matrix $\mathbf{G}_t$ is defined as:

$$\mathbf{G}_t = \begin{bmatrix} 1 & 0 & -(v/w)\cos\theta + (v/w)\cos(\theta+\omega\Delta t) \\ 0 & 1 & -(v/w)\cos\theta + (v/w)\cos(\theta+\omega\Delta t) \\ 0 & 0 & 1 \end{bmatrix} \tag{6}$$

The update step refines the predicted state based on actual measurements. The Kalman gain ($\mathbf{K}_t$) is calculated, and the state estimate is updated accordingly:

$$\mathbf{K}_t = \mathbf{P}_t^- \mathbf{H}_t^T (\mathbf{H}_t \mathbf{P}_t^- \mathbf{H}_t^T + \mathbf{Q}_t)^{-1} \tag{7}$$

$$\hat{\mathbf{x}}_t = \hat{\mathbf{x}}_t^- + \mathbf{K}_t(\mathbf{z}_t - h(\hat{\mathbf{x}}_t^-)) \tag{8}$$

$$\mathbf{P}_t = (\mathbf{I} - \mathbf{K}_t\mathbf{H}_t)\mathbf{P}_t^- \tag{9}$$

Here, $\mathbf{H}_t$ is the Jacobian matrix of the measurement model, and $\mathbf{I}$ is the identity matrix. The measurement Jacobian $\mathbf{H}_t$ is defined as:

$$\mathbf{H}_t = \begin{bmatrix} 1 & 0 & 0 \\ 0 & 1 & 0 \end{bmatrix} \tag{10}$$

The EKF algorithm iteratively applies these steps for each new measurement, ensuring a continuous refinement of the system state estimation.

3.5 Unscented Kalman Filter Implementation

In this section, the implementation of the Unscented Kalman Filter (UKF) for estimating the system state is presented, encompassing the vehicle's position (x, y) and orientation (θ). The UKF begins by generating sigma points $(\mathscr{X}_t)$ to capture the distribution of possible states:

$$\mathscr{X}_t = [\mathbf{x}_t, \mathbf{x}_t + \sqrt{(n+\lambda)\mathbf{P}_t}, \mathbf{x}_t - \sqrt{(n+\lambda)\mathbf{P}_t}] \tag{11}$$

Here, n represents the dimension of the state vector, and λ is a scaling parameter. With a 3-dimensional state, there are a total of 7 sigma points. In the prediction step, each sigma point undergoes propagation through the motion model, resulting in predicted sigma points:

$$\mathscr{Y}_t = f(\mathscr{X}_t, \mathbf{u}_t, \Delta t) \tag{12}$$

These predicted sigma points $(\mathscr{Y}_t)$ are then employed to calculate the predicted mean $(\hat{\mathbf{x}}_t^-)$ and covariance matrix $(\mathbf{P}_t^-)$:

$$\hat{\mathbf{x}}_t^- = \sum_{i=0}^{2n} w_i \mathscr{Y}_{t,i} \tag{13}$$

$$\mathbf{P}_t^- = \sum_{i=0}^{2n} w_i (\mathscr{Y}_{t,i} - \hat{\mathbf{x}}_t^-)(\mathscr{Y}_{t,i} - \hat{\mathbf{x}}_t^-)^T + \mathbf{R}_t \tag{14}$$

Here, w_i denotes the weights assigned to each sigma point, and $\mathbf{R}_t$ is the process noise covariance matrix. The weight for the first sigma point is $\frac{\lambda}{n+\lambda}$, and for the other points, it is $\frac{1}{2(n+\lambda)}$. Additionally, the covariance is adjusted by $(1+\alpha^2+\beta)$ for the first weight.

Moving on to the measurement update step, predicted sigma points $(\mathscr{Y}_t)$ are employed to compute the predicted measurements:

$$\mathscr{Z}_t = h(\mathscr{Y}_t) \tag{15}$$

These predicted measurements $(\mathscr{Z}_t)$ are then utilized to calculate the predicted mean measurement $(\hat{\mathbf{z}}_t)$ and covariance matrix $(\mathbf{S}_t)$:

$$\hat{\mathbf{z}}_t = \sum_{i=0}^{2n} w_i \mathscr{Z}_{t,i} \tag{16}$$

$$\mathbf{S}_t = \sum_{i=0}^{2n} w_i (\mathscr{Z}_{t,i} - \hat{\mathbf{z}}_t)(\mathscr{Z}_{t,i} - \hat{\mathbf{z}}_t)^T + \mathbf{Q}_t \tag{17}$$

The cross-covariance matrix $(\mathbf{P}_{xy})$ is computed as:

$$\mathbf{P}_{xy} = \sum_{i=0}^{2n} w_i (\mathscr{Y}_{t,i} - \hat{\mathbf{x}}_t^-)(\mathscr{Z}_{t,i} - \hat{\mathbf{z}}_t)^T \tag{18}$$

Finally, the Kalman gain ($\mathbf{K}_t$), updated state estimate ($\hat{\mathbf{x}}_t$), and updated covariance matrix ($\mathbf{P}_t$) are calculated as:

$$\mathbf{K}_t = \mathbf{P}_{xy}\mathbf{S}_t^{-1} \tag{19}$$

$$\hat{\mathbf{x}}_t = \hat{\mathbf{x}}_t^- + \mathbf{K}_t(\mathbf{z}_t - \hat{\mathbf{z}}_t) \tag{20}$$

$$\mathbf{P}_t = \mathbf{P}_t^- - \mathbf{K}_t\mathbf{S}_t\mathbf{K}_t^T \tag{21}$$

Here, h represents the measurement model function, w_i are the weights, and $\mathbf{Q}_t$ is the measurement noise covariance matrix. The UKF algorithm iteratively applies these steps for each new measurement, ensuring a robust and accurate estimation of the system state.

3.6 Performance evaluation metric

The Root Mean Square Error (RMSE) stands out as a widely utilized evaluation metric, especially in fields like robotics and localization, where assessing the accuracy of estimation results is crucial. It offers a holistic measure by considering both bias and variance. Particularly well-suited for evaluating filter performance in applications such as estimating a vehicle's position (x, y) [5], RMSE is calculated in the same units as the measured variable, ensuring mathematical convenience and widespread acceptance in the scientific community. The formula for RMSE is expressed as:

$$RMSE = \sqrt{\frac{1}{N}\sum_{i=1}^{N}(\mathbf{y_i} - \hat{\mathbf{y}}_\mathbf{i})^2} \tag{22}$$

In this equation, $\mathbf{y_i}$ represents the ground truth value, and $\hat{\mathbf{y}}_\mathbf{i}$ is the estimated value. When applied to compare the estimation results of the Extended Kalman Filter (EKF) and Unscented Kalman Filter (UKF) in the given system, RMSE emerges as a robust metric. Its sensitivity to large errors allows it to penalize significant deviations between estimated and true values, providing a comprehensive assessment of performance. The ease of calculation, widespread acceptance, and its ability to facilitate a straightforward comparison make RMSE a meaningful and practical metric for evaluating the overall performance of EKF and UKF in the specified context.

4 Results and Analysis

For this experiment, we selected six distinct datasets from the KITTI dataset [4]. I applied the previously mentioned EKF and UKF algorithms to all six datasets and analyzed their performance. In Figure 1, the results of both estimation methods under two scenarios are presented: high noise and low noise (Q and R). The first three datasets were collected over a short time, while the last three were collected over a longer duration. Both estimation methods exhibit poorer performance as the noise level increases, but the analysis indicates that the EKF outperforms the UKF.

Subsequently, attention is directed towards the yaw angle state, as it remains unobserved in the system. Using the identical datasets and configuration, the ground truth and estimated yaw angles are depicted in Figure 2. An analysis of this figure reveals a superior performance of the EKF compared to the UKF, especially when a specific state is unobserved.

(a) Dataset 2011_09_26_0019

(b) Dataset 2011_09_26_0023

(c) Dataset 2011_09_26_0035

(d) Dataset 2011_09_30_0020

(e) Dataset 2011_09_30_0033

(f) Dataset 2011_09_30_0034

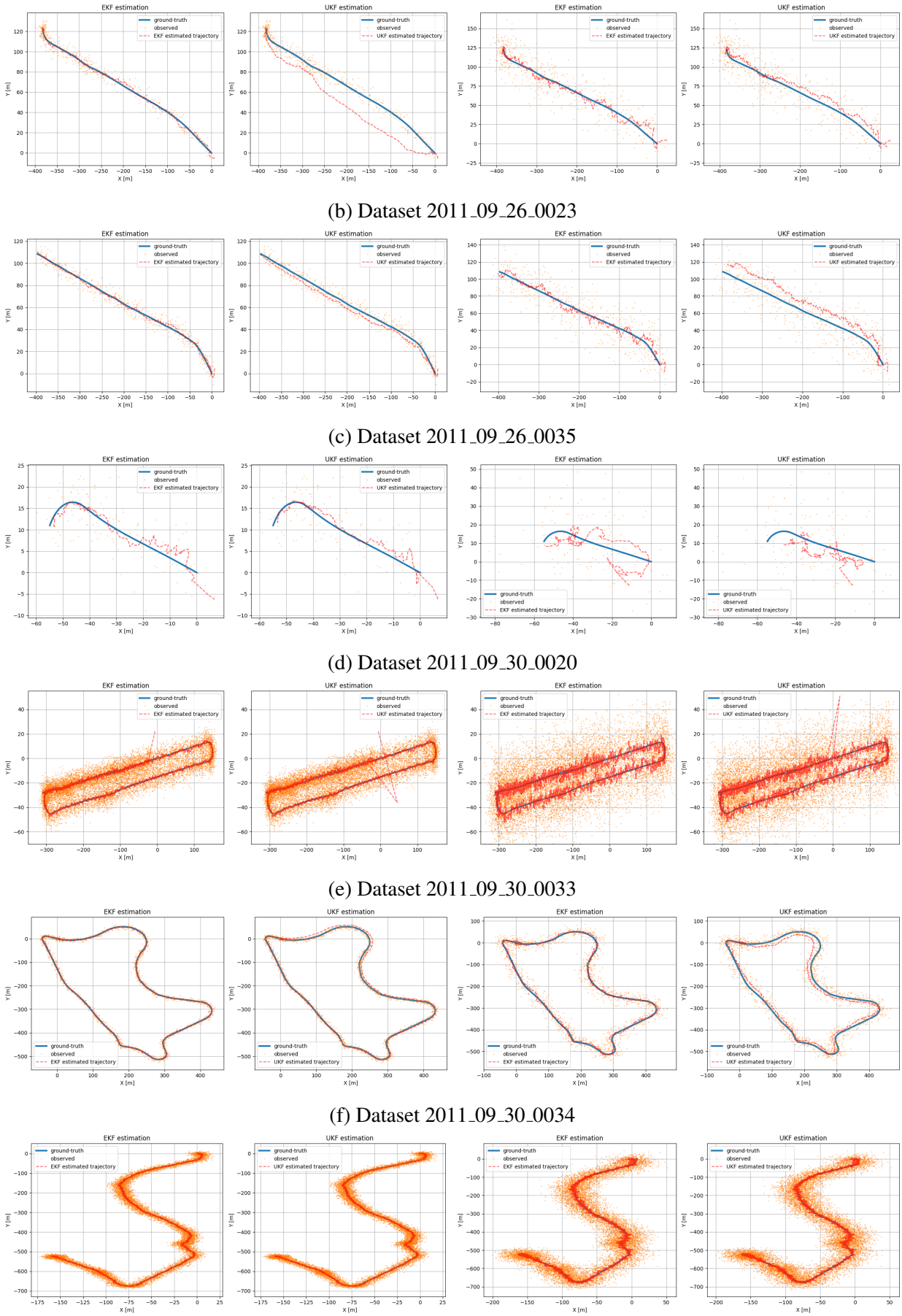

Figure 1: Comparison of EKF and UKF estimation results for different dataset (low Q and R)
Left subplot: Low Q and R; Right subplot: High Q and R

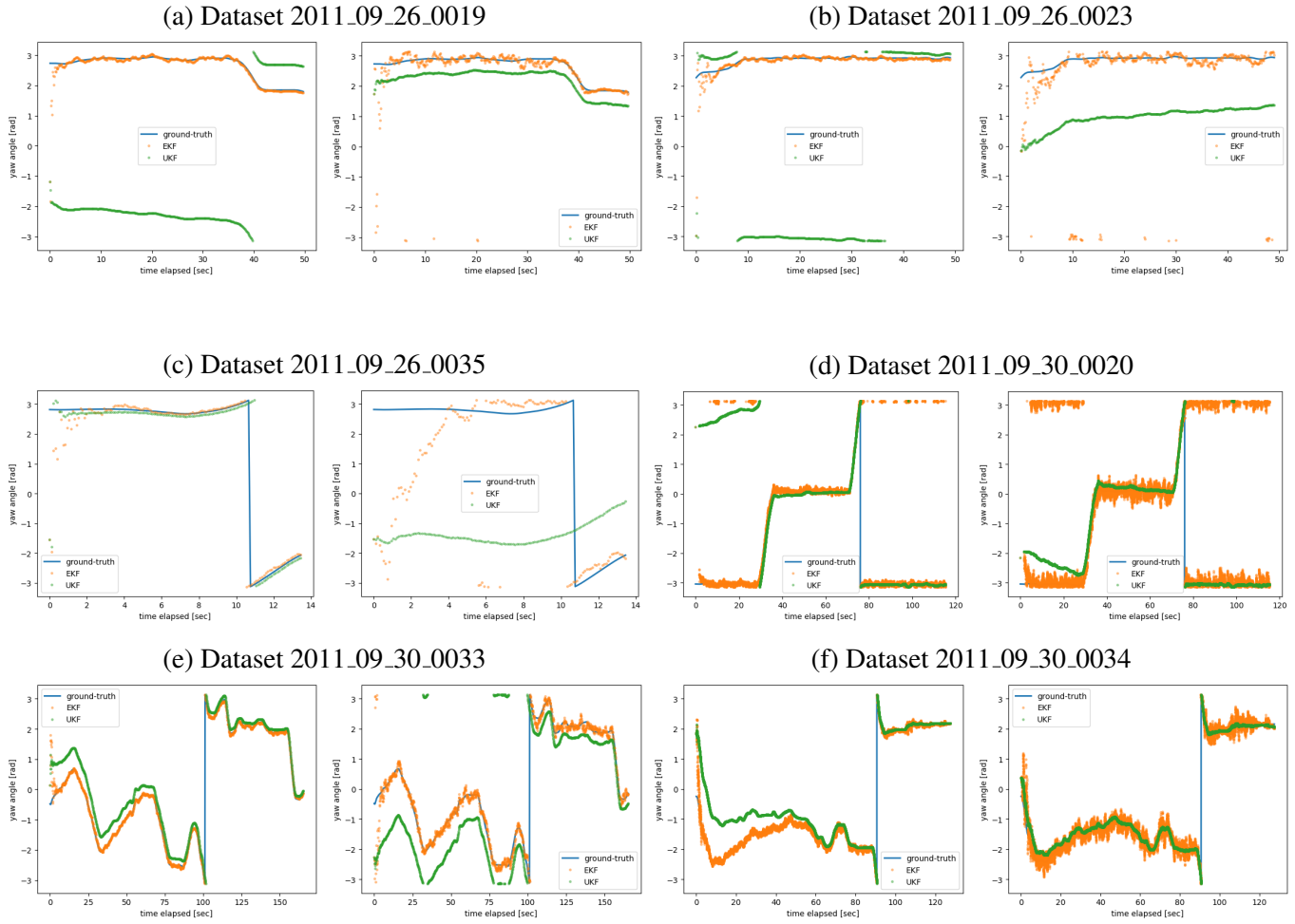

Figure 2: Comparison of EKF and UKF estimation results for different dataset (low Q and R)
Left subplot: Low Q and R; Right subplot: High Q and R

Table 1 presents the Root Mean Square Error (RMSE) calculations for the ground-truth values and the estimated values obtained from both the Extended Kalman Filter (EKF) and the Unscented Kalman Filter (UKF) for all three state variables, namely x, y, and θ, under both low and high noise conditions. The RMSE serves as a quantitative evaluation metric for comparing the accuracy of these values.

Generally, the estimators demonstrate superior performance in low noise scenarios compared to high noise scenarios, as is typical in evaluation metrics. However, it's noteworthy that this trend is more pronounced in the case of the EKF, although there are instances where the UKF exhibits better results in high noise conditions, such as in Dataset 2011_09_25_0019.

Nevertheless, when conducting a direct comparison between the EKF and UKF in our specific scenario, the EKF consistently outperforms the UKF across various datasets and noise levels. This can be observed from the Table 1.

Table 1: RMSE Analysis for EKF and UKF

Dataset name	EKF (low noise)	UKF (low noise)	EKF (high noise)	UKF (high noise)
2011_09_26_0019	x: 1.068 y: 1.580 θ: 0.189	x: 4.560 y: 15.978 θ: 1.120	x: 2.933 y: 4.609 θ: 0.257	x: 4.860 y: 4.894 θ: 0.458
2011_09_26_0023	x: 1.085 y: 1.422 θ: 0.166	x: 0.806 y: 3.726 θ: 0.322	x: 3.048 y: 4.189 θ: 0.356	x: 17.166 y: 7.850 θ: 1.910
2011_09_26_0035	x: 1.038 y: 1.491 θ: 0.362	x: 1.401 y: 1.114 θ: 0.245	x: 6.693 y: 4.573 θ: 1.052	x: 8.360 y: 6.047 θ: 1.936
2011_09_30_0020	x: 0.857 y: 0.974 θ: 0.612	x: 1.092 y: 1.073 θ: 0.316	x: 2.529 y: 2.911 θ: 0.182	x: 2.934 y: 2.724 θ: 0.371
2011_09_30_0033	x: 1.428 y: 1.343 θ: 0.165	x: 3.536 y: 3.797 θ: 0.407	x: 3.855 y: 3.373 θ: 0.325	x: 9.071 y: 8.995 θ: 0.909
2011_09_30_0034	x: 0.912 y: 0.873 θ: 0.164	x: 1.029 y: 0.904 θ: 0.657	x: 2.708 y: 2.777 θ: 0.213	x: 2.612 y: 2.859 θ: 0.141

5 Conclusion

In summary, this research centered on implementing the Extended Kalman Filter (EKF) and Unscented Kalman Filter (UKF) algorithms for estimating state variables utilizing datasets from the KITTI dataset. The control inputs comprised forward velocity and angular velocity with direct measurements of position states, while the orientation remained unobserved. The investigation covered scenarios with varying levels of noise.

The comparative analysis revealed consistent superiority of the EKF over the UKF across different datasets and noise levels, especially in cases where certain states, such as the yaw angle, were unobserved. The EKF demonstrated a more robust and reliable performance within our specific analytical context, findings supported by quantitative assessments using Root Mean Square Error (RMSE) calculations.

Despite existing literature generally favoring the UKF over the EKF, our results presented a contrasting perspective. This discrepancy appears to be associated with the system's complexity, where the performance of these methods is heavily influenced by the intricacies of non-linearity. In our research, the motion model's non-linearity is less complex, and the measurement model is linear. This reduced complexity contributes to a more accurate approximation of non-linearity, resulting in superior estimation outcomes for the EKF. In contrast, the UKF's use of sigma points to capture value distribution introduces inaccuracies, leading to suboptimal results.

To conclude, our findings indicate that, under the specific conditions of our study, the Extended Kalman Filter emerges as a more effective and reliable choice compared to the Unscented Kalman Filter, particularly when dealing with relatively simple non-linear systems. These insights contribute valuable considerations for the selection of estimation algorithms in similar applications.

References

[1] C. Raveena, R. Sravya, R. Kumar, and A. Chavan, "Sensor fusion module using imu and gps sensors for autonomous car," in *2020 IEEE International Conference for Innovation in Technology (INOCON)*, 2020. doi: 10.1109/INOCON50539.2020.9298316 pp. 1–6.

[2] M. I. Ribeiro, "Kalman and extended kalman filters: Concept, derivation and properties," *Institute for Systems and Robotics*, vol. 43, no. 46, pp. 3736–3741, 2004.

[3] E. Wan and R. Van Der Merwe, "The unscented kalman filter for nonlinear estimation," in *Proceedings of the IEEE 2000 Adaptive Systems for Signal Processing, Communications, and Control Symposium (Cat. No.00EX373)*, 2000. doi: 10.1109/ASSPCC.2000.882463 pp. 153–158.

[4] A. Geiger, P. Lenz, C. Stiller, and R. Urtasun, "Vision meets robotics: The kitti dataset," *International Journal of Robotics Research (IJRR)*, 2013.

[5] S. Konatowski, P. Kaniewski, and J. Matuszewski, "Comparison of estimation accuracy of ekf, ukf and pf filters," *Annual of Navigation*, no. 23, pp. 69–87, 2016.

[6] A. Giannitrapani, N. Ceccarelli, F. Scortecci, and A. Garulli, "Comparison of ekf and ukf for spacecraft localization via angle measurements," *IEEE Transactions on aerospace and electronic systems*, vol. 47, no. 1, pp. 75–84, 2011.

[7] B. Allotta, L. Chisci, R. Costanzi, F. Fanelli, C. Fantacci, E. Meli, A. Ridolfi, A. Caiti, F. Di Corato, and D. Fenucci, "A comparison between ekf-based and ukf-based navigation algorithms for auvs localization," in *OCEANS 2015-Genova*. IEEE, 2015, pp. 1–5.

[8] P. Chhetri, "Kitti dataset readme," https://github.com/pratikac/kitti/blob/master/readme.raw.txt, accessed: January 14, 2024.

[9] S. Thrun, W. Burgard, and D. Fox, *Probabilistic Robotics*. MIT Press, 2005.

[10] B. Hofmann-Wellenhof, H. Lichtenegger, and J. Collins, *Global positioning system: theory and practice*. Springer Science & Business Media, 2012.